fractal and fractional

MDPI

Article

Characteristics of New Stochastic Solitonic Solutions for the Chiral Type of Nonlinear Schrödinger Equation

H. G. Abdelwahed [1,2,*], A. F. Alsarhana [1], E. K. El-Shewy [2,3] and Mahmoud A. E. Abdelrahman [4,5]

[1] Department of Physics, College of Science and Humanities, Al-Kharj, Prince Sattam bin Abdulaziz University, Al-Kharj 11942, Saudi Arabia
[2] Theoretical Physics Group, Faculty of Science, Mansoura University, Mansoura 35516, Egypt
[3] Department of Physics, College of Science, Taibah University, Al-Madinah Al-Munawarah 30001, Saudi Arabia
[4] Department of Mathematics, College of Science, Taibah University, Al-Madinah Al-Munawarah 30001, Saudi Arabia
[5] Department of Mathematics, Faculty of Science, Mansoura University, Mansoura 35516, Egypt
* Correspondence: h.abdelwahed@psau.edu.sa or hgomaa_eg@mans.edu.eg

Abstract: The Wiener process was used to explore the (2 + 1)-dimensional chiral nonlinear Schrödinger equation (CNLSE). This model outlines the energy characteristics of quantum physics' fractional Hall effect edge states. The sine-Gordon expansion technique (SGET) was implemented to extract stochastic solutions for the CNLSE through multiplicative noise effects. This method accurately described a variety of solitary behaviors, including bright solitons, dark periodic envelopes, solitonic forms, and dissipative and dissipative–soliton-like waves, showing how the solutions changed as the values of the studied system's physical parameters were changed. The stochastic parameter was shown to affect the damping, growth, and conversion effects on the bright (dark) envelope and shock-forced oscillatory wave energy, amplitudes, and frequencies. In addition, the intensity of noise resulted in enormous periodic envelope stochastic structures and shock-forced oscillatory behaviors. The proposed technique is applicable to various energy equations in the nonlinear applied sciences.

Keywords: Wiener process; chiral NLSE; nonlinearity structures; stochastic solitons

Citation: Abdelwahed, H.G.; Alsarhana, A.F.; El-Shewy, E.K.; Abdelrahman, M.A.E. Characteristics of New Stochastic Solitonic Solutions for the Chiral Type of Nonlinear Schrödinger Equation. *Fractal Fract.* **2023**, *7*, 461. https://doi.org/10.3390/fractalfract7060461

Academic Editors: Riccardo Caponetto, Mohammad Partohaghighi and Ali Akgül

Received: 11 April 2023
Revised: 13 May 2023
Accepted: 21 May 2023
Published: 5 June 2023

1. Introduction

The important features of new solitonic envelopes form a foundation for the novel scientific energy universe, which is of great importance for a number of disciplines, including plasma physics, solid-state physics, telecommunications, superfluidity, quantum mechanics, and astrophysical dynamics [1–6]. These types of solution have attracted particular attention from physicists, mathematicians, and engineers [7–12]. Several new analytical methods, such as the $(\frac{G'}{G})$—expansion approach, sub-equation approach, enhanced modified extended tanh-expansion approach have been used to obtain several nonlinear energy structures, which have been used to investigate the influence of physical parameters on energy and wave properties [13–15]. However, in recent decades there has been significant interest in understanding energy equations via the study of nonlinear Schrödinger equation dynamics in nature [16,17].

The investigation of chiral wave structures has a significant role in the developments of quantum mechanisms, specially in Hall-effect applications. Biswas obtained topological and nontopological solitons for a chiral NLSE model with time-dependent and constant coefficients [18]. Alharbi et al. investigated the dynamical Brownian stochastic CNLSE in two dimensions [19]. It was noted that the random noise parameter modulated the solitonic structures. Moreover, the Brownian noise affected the solitary features and produced distorted beak oscillatory shocks. Javid and Raza [20], explained the dark and singular solitons obtained from the (1 + 2) CNLSE using an M-simple-equation and the $\exp(-\varphi(\xi))$-expansion methods. It was reported that the solution movements and phase shift mainly

depended on the signs of the equation constants. Eslami [21] studied the (1 + 2) CNLSE solutions using a trial solution technique. It was noted that, in this model, the stationary and singular soliton were retrieved. In addition, the structures were produced via constraint conditions for the equation coefficients.Recently, due to its increasingly widespread application, numerous analytical and numerical techniques have been developed for deterministic and stochastic NPDEs, such as the unified solver approach [22], Crank–Nicolson method [23], improved modified extended tanh-function method [24], implicit meshless method [25], finite difference method [26], adaptive moving mesh method [27], and operational matrix method [28].

The dominant model considered in this work is the (2 + 1)-dimensional CNLSE using a noise term. In this investigation, the nonlinear Schrödinger equations (NLSEs) were restricted using random noise effects, which have important nonlinear energy applications in superfluidity, quantum mechanics, plasma space, optical fibers, and other fields of science. The NLSE is described as wave propagations affected by the Kerr effect, dispersion, and group velocity. The solitonic solutions for NLSEs become important in nonlinearity energy studies. Recently, the NLSEs forced or damped with random noises using stochastic soliton solutions have become an important representative tool for explaining the propagations of a wave in solid state physics, chemical engineering, fiber communications, nuclear physics, and solid-state and energy physics [29–31].

We consider the $(2+1)$-dimensional CNLSE [20,21]:

$$i\Psi_t + \alpha(\Psi_{xx} + \Psi_{yy}) + i\Big(c_1\Psi(\Psi\Psi_x^* - \Psi^*\Psi_x) + c_2\Psi(\Psi\Psi_y^* - \Psi^*\Psi_y)\Big) - i\sigma\,\Psi\,\mathrm{Y}_t = 0, \quad (1)$$

$\Psi = \Psi(x, y, t)$ denotes a complex function in time t and the directions x, y, and α are the coefficient of dispersion; c_1 & c_2 denote the coefficients of the nonlinear coupling terms; and σ denotes the noise strength. Y_t represents the time derivative of the Wiener process $\mathrm{Y}(t)$ [32]. Equation (1) cannot be integrated using the inverse scattering transform approach because it fails the Painleve integrability condition. It is also worth noting that Equation (1) is not invariant under Galilean transformation. There have been several studies carried out for Equation (1) when there is no stochastic influence [21,33–36].

In the present research, by using the sine-Gordon expansion approach, we provide some important stochastic solutions to the 2D CNLSE induced by multiplicative noise in the Itô sense. The suggested technique offers a number of benefits, including the ability to use freely physical parameters to deliver accurate solutions in an explicit form. Clarifying the impact of the noise on the obtained solutions is one of the most intriguing points. We also show how certain chosen stochastic solutions affected the nonlinear dynamics of the model. To the best of our knowledge, no one has ever utilized the proposed technique to solve the (2 + 1)-dimensional CNLSE in the Itô sense.

This paper is structured as follows: Section 2 introduces a description of the proposed method and the Wiener process. Section 3 provides the stochastic solutions to the 2D stochastic CNLSE. Section 4 presents an explanation of the gained stochastic solution. The conclusions are summarized in Section 5.

2. Preliminaries

In this section we introduce the abbreviation of the sine-Gordon expansion approach [37] and the Wiener process.

2.1. Description of the Method

Consider the sine-Gordon equation [37]

$$\Psi_{xx} - \Psi_{tt} = \delta^2 \sin(\Psi), \quad (2)$$

where $\Psi(x, t)$ and δ is a non-zero real number. Utilizing the wave transform

$$\Psi(x, t) = \Phi(\zeta), \zeta = x - wt. \quad (3)$$

Equation (2) is reduced to

$$\Phi'' = \frac{\delta^2}{1-w^2}\sin(\Phi). \tag{4}$$

Multiplying Φ' on both sides of Equation (4) and integrating it one time yields

$$\left[\left(\frac{\Phi}{2}\right)'\right]^2 = \frac{\delta^2}{1-w^2}\sin^2(\frac{\Phi}{2}) + K, \tag{5}$$

K is the constant of integration. Setting $K = 0$, $\frac{\Phi}{2} = \psi(\zeta)$ and $\frac{\delta^2}{1-w^2} = a^2$ into Equation (5) yields

$$\psi' = a\sin(\psi). \tag{6}$$

Choosing $a = 1$, Equation (6) becomes

$$\psi' = \sin(\psi). \tag{7}$$

The solution of Equation (7) is given as follows:

$$\sin(\psi) = \sin(\psi(\zeta)) = \frac{2Ke^{\zeta}}{K^2\,e^{2\zeta}+1}\;|_{K=1} = \operatorname{sech}(\zeta). \tag{8}$$

$$\cos(\psi) = \cos(\psi(\zeta)) = \frac{K^2e^{2\zeta}-1}{K^2\,e^{2\zeta}+1}\;|_{K=1} = \tanh(\zeta). \tag{9}$$

Now, consider the following NPDEs:

$$\mathcal{H}(\Psi, \Psi_x, \Psi_t, \Psi_{xx}, \Psi_{xt}, \Psi_{tt}, \ldots) = 0. \tag{10}$$

Using the wave transformation:

$$\Psi(x,t) = \Phi(\zeta), \qquad \zeta = x - w\,t,$$

w is the wave speed, Equation (10) is reduced to the following ODE:

$$\mathcal{G}(\Phi, \Phi', \Phi'', \Phi''', \ldots) = 0. \tag{11}$$

It is assumed that the solution $\Phi(\zeta)$ of Equation (11) can be written as

$$\Phi(\zeta) = \sum_{i=1}^{N} \tanh^{i-1}(\zeta)[B_i\operatorname{sech}(\zeta) + A_i\tanh(\zeta)] + A_0. \tag{12}$$

Considering Equations (8) and (9), Equation (12) can be written as follows:

$$\Phi(\psi) = \sum_{i=1}^{N} \cos^{i-1}(\psi)[B_i\sin(\psi) + A_i\cos(\psi)] + A_0. \tag{13}$$

The value of N is determined by utilizing the homogeneous balance principle. Superseding Equation (13) into Equation (11), and comparing the terms, yields a system of algebraic equations. Solving these equations, gives the traveling wave solutions of Equation (10).

2.2. Wiener Process

A stochastic process is a mathematical model of the possible future manifestations of a random phenomena when it first occurs [38]. The Wiener process is an example of a continuous-time stochastic process. This process meets the following requirements:

(i) $\Upsilon(t)$ is a continuous functions of $t \geq 0$,
(ii) For $s < t$, $\Upsilon(s) - \Upsilon(t)$ is independent of increments,

(iii) $\Upsilon(t) - \Upsilon(s)$ has a normal distribution through mean 0 and variance $t - s$.

The distributional derivative of the Wiener process $\dot{\Upsilon} = \Upsilon_t = \frac{d\Upsilon}{dt}$ is the white noise in time. It is delta correlated in the sense that

$$\mathbb{E}(\dot{\Upsilon}(t)\dot{\Upsilon}(r)) = \delta_{t-r},$$

δ is the Dirac mass. As the Dirac mass has a constant Fourier transform, the term "white noise" was coined. White noise is frequently thought of as a mathematical idealization of occurrences such as sudden, large fluctuations. It should be underlined that the Itô lemma is used to calculate the time derivative of stochastic processes as follows:

$$d\chi = \chi(\Upsilon_{t+dt}, t + dt) \; - \; \chi(\Upsilon_t, t),$$

where $\chi(\Upsilon_t, t)$ represents the time derivative of stochastic processes, while $\chi(\Upsilon, t)$ denotes a differentiable function. Thus, this illustrates how χ has changed in a short amount of time dt. The Itô lemma for the Wiener process is represented as

$$d\chi(\Upsilon_t, t) = \partial_\Upsilon \chi(\Upsilon_t, t)\, d\Upsilon_t + \frac{1}{2}\, \partial_\Upsilon^2\, \chi(\Upsilon_t, t)\, dt \; + \; \partial_t\, \chi(\Upsilon_t, t)\, dt.$$

One can construct the stochastic integral $\int_0^t \Psi(\theta) d\Upsilon(\theta)$ in a variety of ways. The most familiar types of a stochastic integral are those by Itô and Stratonovich. When the integral is calculated at the left-end point, it is said to have an Itô stochastic integral. When the stochastic integral is calculated at the midpoint, it is referred to as a Stratonovich stochastic integral [39].

3. The Stochastic Solutions for Equation (1)

Utilizing wave transformation [20]:

$$\Psi(t, x) = \psi(\rho) e^{i\theta + \sigma\Upsilon(t) - \sigma^2 t}, \quad \rho = \rho_1 x + \rho_2 y - \rho_3 t, \quad \theta = \theta_1 x + \theta_2 y + \theta_3 t + \varepsilon, \tag{14}$$

θ_1, θ_2, denote the frequencies in x and y directions, θ_3 and ε symbolize the soliton frequency and phase constant. In addition, ρ_1 and ρ_2 are wave numbers in x and y directions and ρ_3 is a traveling velocity.

Setting Equation (14) into Equation (1) produces

$$-\sigma^2 \psi + (-\rho_3 + 2\alpha(\rho_1\theta_1 + \rho_2\theta_2))\psi' = 0 \tag{15}$$

for the imaginary part and

$$L\, \psi'' + M\, \psi^3 + N\, \psi = 0 \tag{16}$$

for the real part, $L = \alpha(\rho_1^2 + \rho_2^2)$, $M = 2(c_1\theta_1 + c_2\theta_2)$ and $N = -(\alpha(\theta_1^2 + \theta_2^2) + \theta_3)$. Equation (16) provides the soliton solutions under the condition

$$\alpha\sigma^4 \left(\rho_1^2 + \rho_2^2\right) e^{-\frac{2\rho\sigma^2}{2\alpha\theta_1\rho_1 + 2\alpha\theta_2\rho_2 - \rho_3}} + 2(c_1\theta_1 + c_2\theta_2)(\rho_3 - 2\alpha(\theta_1\rho_1 + \theta_2\rho_2))^2 = 0. \tag{17}$$

Balancing the highest order derivative term ψ'' and highest nonlinear term ψ^3 in Equation (16) yields $N = 1$. Thus, the solution of Equation (16) takes the form:

$$\psi(\rho) = \Lambda_0 + \Lambda_1 \tanh(\rho) + \Gamma_1 \operatorname{sech}(\rho). \tag{18}$$

Substituting ψ, ψ'', and ψ^3 into Equation (16) and setting the coefficients of the hyperbolic functions to zero produces a system of algebraic equations, which yields

Family I:

The stochastic solutions of Equation (16) are

$$\psi_{1,2}(x,y,t) = \pm\sqrt{\frac{-\alpha(\rho_1^2+\rho_2^2)}{\theta_1 c_1+\theta_2 c_2}}\tanh(\rho_1 x+\rho_2 y-\rho_3 t)\,. \tag{19}$$

Thus, the stochastic dark solutions for Equation (1) are

$$\Psi_{1,2}(x,y,t) = \pm\sqrt{\frac{-\alpha(\rho_1^2+\rho_2^2)}{\theta_1 c_1+\theta_2 c_2}}\tanh(\rho_1 x+\rho_2 y-\rho_3 t)\,e^{i(\theta_1 x+\theta_2 y+\theta_3 t+\varepsilon)+\sigma\Upsilon(t)-\sigma^2 t}\,, \tag{20}$$

$\theta_3 = -\alpha(2(\rho_1^2+\rho_2^2)+\theta_1^2+\theta_2^2)$, $\theta_1 c_1+\theta_2 c_2 \neq 0$.

Family II:

The stochastic solutions of Equation (16) are

$$\psi_{3,4}(x,y,t) = \pm\sqrt{\frac{\alpha(\rho_1^2+\rho_2^2)}{\theta_1 c_1+\theta_2 c_2}}\operatorname{sech}(\rho_1 x+\rho_2 y-\rho_3 t)\,. \tag{21}$$

Hence, the stochastic bright solutions for Equation (1) are

$$\Psi_{3,4}(x,y,t) = \pm\sqrt{\frac{\alpha(\rho_1^2+\rho_2^2)}{\theta_1 c_1+\theta_2 c_2}}\operatorname{sech}(\rho_1 x+\rho_2 y-\rho_3 t)\,e^{i(\theta_1 x+\theta_2 y+\theta_3 t+\varepsilon)+\sigma\Upsilon(t)-\sigma^2 t}\,, \tag{22}$$

$\theta_3 = -\alpha(\theta_1^2+\theta_2^2-(\rho_1^2+\rho_2^2))$, $\theta_1 c_1+\theta_2 c_2 \neq 0$.

Family III:

The stochastic solutions of Equation (16) are

$$\psi_{5,6}(x,y,t) = \pm\sqrt{\frac{-\alpha(\rho_1^2+\rho_2^2)}{\theta_1 c_1+\theta_2 c_2}}(\tanh(\rho_1 x+\rho_2 y-\rho_3 t)+i\operatorname{sech}(\rho_1 x+\rho_2 y-\rho_3 t)). \tag{23}$$

Hence, the stochastic combined dark-bright solutions for Equation (1) are

$$\Psi_{5,6}(x,y,t) = \pm\sqrt{\frac{-\alpha(\rho_1^2+\rho_2^2)}{\theta_1 c_1+\theta_2 c_2}}(\tanh(\rho_1 x+\rho_2 y-\rho_3 t)+i\operatorname{sech}(\rho_1 x+\rho_2 y-\rho_3 t))e^{i(\theta_1 x+\theta_2 y+\theta_3 t+\varepsilon)+\sigma\Upsilon(t)-\sigma^2 t}\,, \tag{24}$$

$\theta_3 = -\frac{1}{2}\alpha(2\theta_1^2+2\theta_2^2+\rho_1^2+\rho_2^2)$, $\theta_1 c_1+\theta_2 c_2 \neq 0$.

4. Results and Discussion

An effective and particular $(2+1)$-dimension CNLSE stochastic solution has been achieved using SGET. Since CNLSE denotes the quantum fractional Hall-effect edge states [40–42]. Thus, new solitary forms have been studied in view of the constants and coefficients α, c_1, c_2 and the strength of noise σ. The perfect constitutional behaviors of solutions obtained for Equation (1) are a dark envelope, periodic envelopes, solitons, localized super soliton, dissipative shock-like, symmetric solitons, oscillatory shocks, etc. In neglecting noise effects, Equation (1) produces the following forms:

$$\Psi_{1,2}(x,y,t) = \pm\sqrt{\frac{-\alpha(\rho_1^2+\rho_2^2)}{\theta_1 c_1+\theta_2 c_2}}\tanh(\rho_1 x+\rho_2 y-\rho_3 t)\,e^{i(\theta_1 x+\theta_2 y+\theta_3 t+\varepsilon)}\,. \tag{25}$$

$$\Psi_{3,4}(x,y,t) = \pm\sqrt{\frac{\alpha(\rho_1^2+\rho_2^2)}{\theta_1 c_1+\theta_2 c_2}}\operatorname{sech}(\rho_1 x+\rho_2 y-\rho_3 t)\,e^{i(\theta_1 x+\theta_2 y+\theta_3 t+\varepsilon)}. \tag{26}$$

$$\Psi_{5,6}(x,y,t) = \pm\sqrt{\frac{-\alpha(\rho_1^2+\rho_2^2)}{\theta_1 c_1+\theta_2 c_2}}(\tanh(\rho_1 x+\rho_2 y-\rho_3 t)+i\operatorname{sech}(\rho_1 x+\rho_2 y-\rho_3 t))e^{i(\theta_1 x+\theta_2 y+\theta_3 t+\varepsilon)}. \tag{27}$$

Here, the 3D solution profiles CNLSE have been informed by the physical values of α, c_1 and c_2 for the absence on σ. In view of Figures 1–10, a 3D plot of the obtained solitary forms with x, y and t is given. Equation (25) describes the dark periodic envelopes, and super and solitonic profiles, as in Figures 1–4. The dynamical behavior of Figure 1 shows that a dark envelope is produced for the x axis and a pure periodic wave for the t axis. In addition, a bright soliton wave is directed at the positive x axis generated in Figure 2. In Figures 3 and 4 a plot of Equation (25) with the x and y axis is shown, and a narrow dissipative wave with symmetric periodic waves in the x, y axis and a bright soliton which is directed toward the negative x axis are given. For solution (26), some new physical description solutions are introduced in Figures 5–8. A bright periodic envelope and a positive solitonic structure directed toward the negative x axis are illustrated in Figures 5 and 6. Some important symmetric compressive-rarefactive solitons are produced for the x and y axis, as shown in Figure 7. In Figure 8, a positive soliton directed at the positive x axis is obtained. For solution (27), a combination of dissipative–soliton waves is created, as seen in Figures 9 and 10. These dissipative behaviors are displayed in a symmetric manner with a solitonic shape, as shown in Figure 9, and in the center of the periodic solitary waves, as seen in Figure 10. The presented simulation diagrams for certain model solutions (1) were produced using Matlab Release 18.

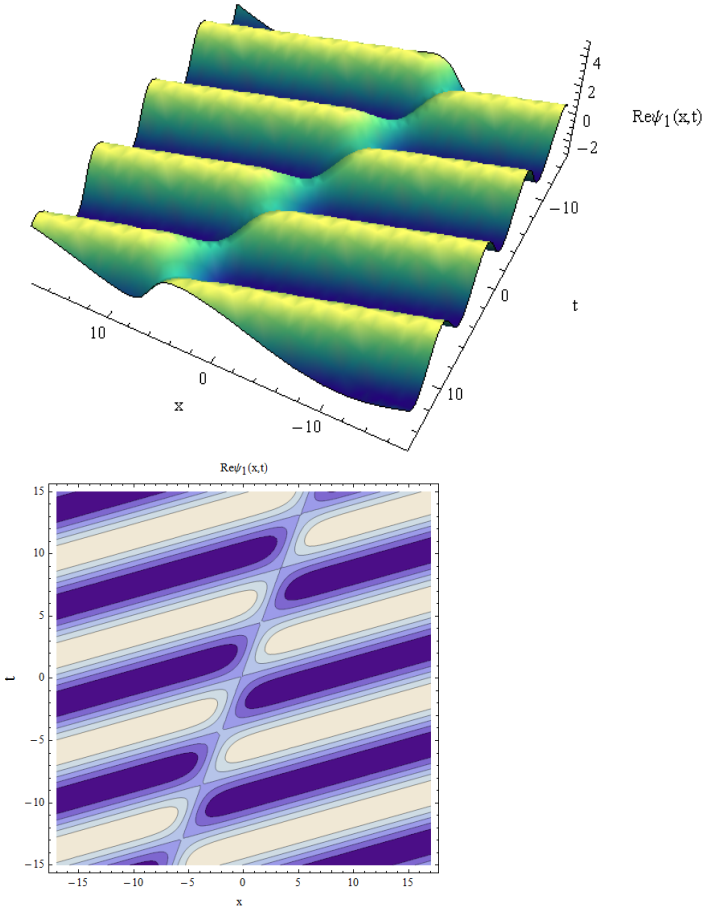

Figure 1. Real part of $\Psi_1(x,t)$ vs. x, t for $\alpha = 0.5$, $\rho_1 = 0.7$, $\rho_2 = 0.5$, $c_1 = 0.4$, $c_2 = 0.3$, $\theta_1 = 0.2$, $\theta_2 = 0.3$, $\varepsilon = 0.05$.

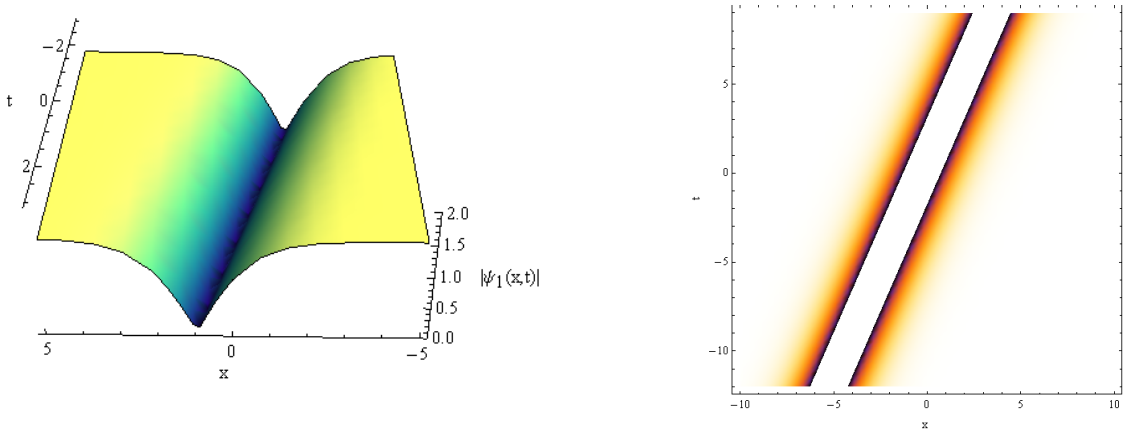

Figure 2. $|\ \Psi_1(x,t)\ |$ vs. x,t for $\alpha = 0.5, \rho_1 = 0.7,\ \rho_2 = 0.5,\ c_1 = 0.4,\ c_2 = 0.3,\ \theta_1 = 0.2, \theta_2 = 0.3,$ $\varepsilon = 0.05$.

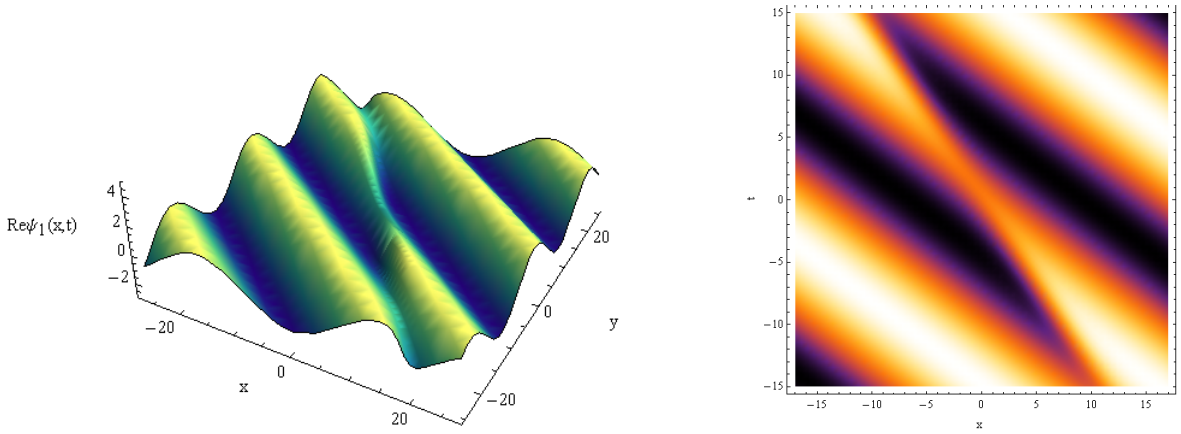

Figure 3. Real part of $\Psi_1(x,t)$ vs. x,y for $\alpha = 0.5,\ \rho_1 = 0.7,\ \rho_2 = 0.5,\ c_1 = 0.4,\ c_2 = 0.3,\ \theta_1 = 0.2,$ $\theta_2 = 0.3, \varepsilon = 0.05$.

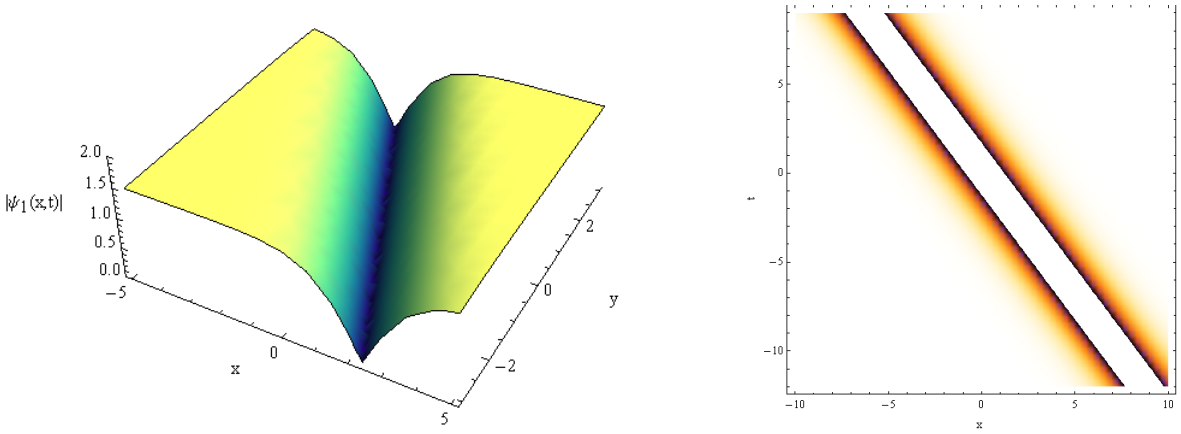

Figure 4. $|\ \Psi_1(x,t)\ |$ vs. x,y for $\alpha = 0.5,\ \rho_1 = 0.7,\ \rho_2 = 0.5,\ c_1 = 0.4,\ c_2 = 0.3, \theta_1 = 0.2,\ \theta_2 = 0.3,$ $\varepsilon = 0.05$.

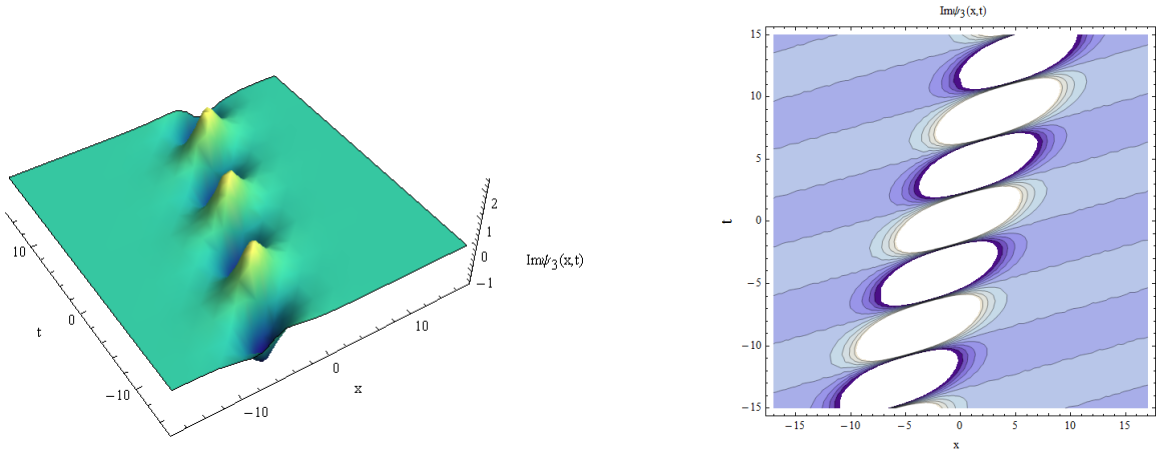

Figure 5. Imaginary part of $\Psi_3(x,t)$ vs. x,t for $\alpha = 0.5$, $\rho_1 = 0.7$, $\rho_2 = 0.5$, $c_1 = 0.4$, $c_2 = 0.3$, $\theta_1 = 0.2$, $\theta_2 = 0.3$, $\varepsilon = 0.05$.

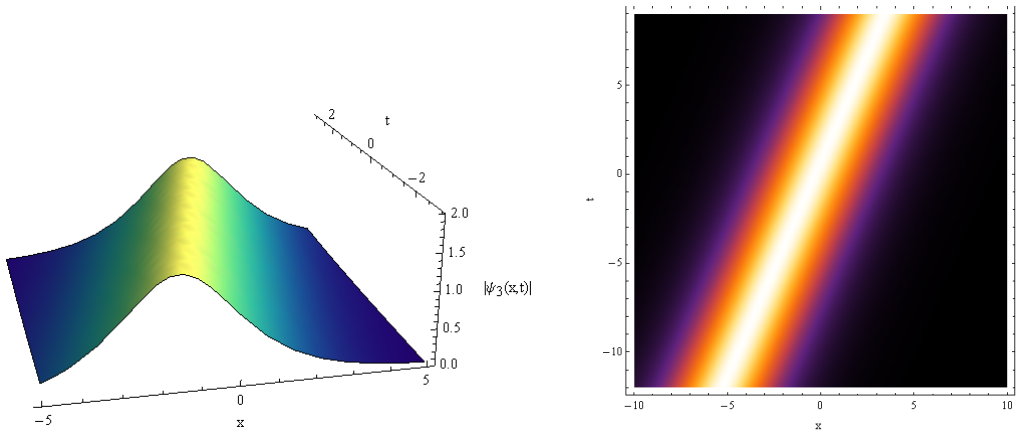

Figure 6. $|\ \Psi_3(x,t)\ |$ vs. x,t for $\alpha = 0.5$, $\rho_1 = 0.7$, $\rho_2 = 0.5$, $c_1 = 0.4$, $c_2 = 0.3$, $\theta_1 = 0.2$, $\theta_2 = 0.3$, $\varepsilon = 0.05$.

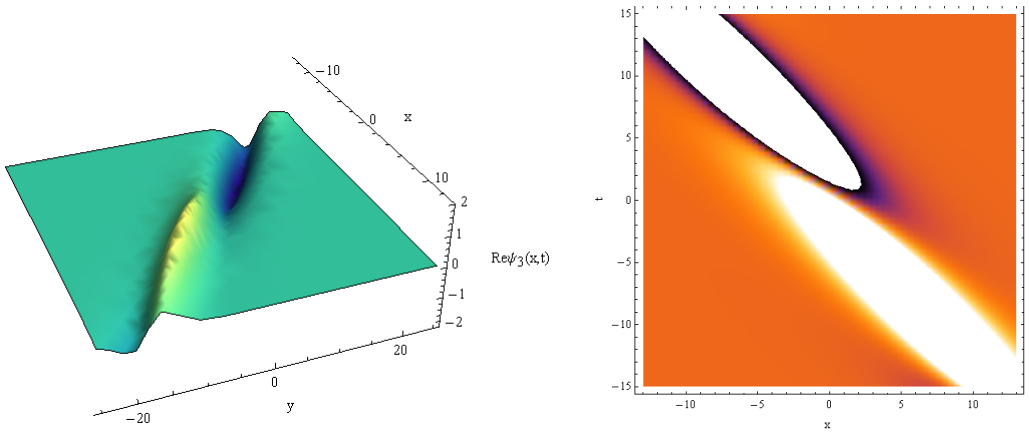

Figure 7. Real part of $\Psi_3(x,t)$ vs. x,y for $\alpha = 0.5$, $\rho_1 = 0.7$, $\rho_2 = 0.5$, $c_1 = 0.4$, $c_2 = 0.3$, $\theta_1 = 0.2$, $\theta_2 = 0.3$, $\varepsilon = 0.05$.

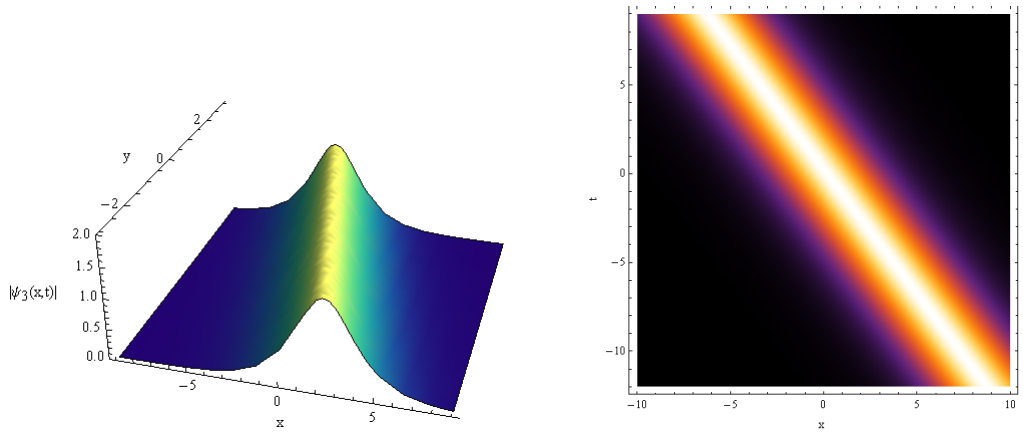

Figure 8. $|\ \Psi_3(x,t)\ |$ vs. x, y for $\alpha = 0.5$, $\rho_1 = 0.7$, $\rho_2 = 0.5$, $c_1 = 0.4$, $c_2 = 0.3$, $\theta_1 = 0.2$, $\theta_2 = 0.3$, $\varepsilon = 0.05$.

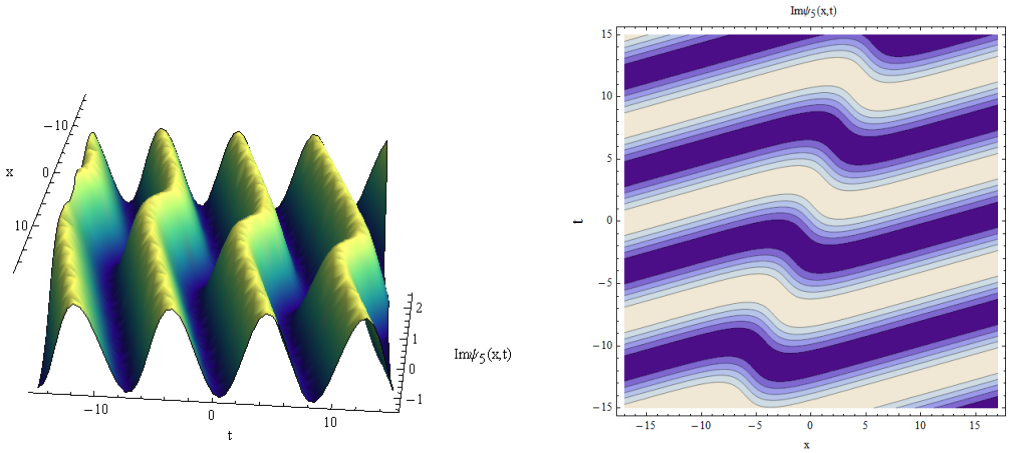

Figure 9. Imaginary part of $\Psi_5(x,t)$ vs. x, t for $\alpha = 0.5$, $\rho_1 = 0.7$, $\rho_2 = 0.5$, $c_1 = 0.4$, $c_2 = 0.3$, $\theta_1 = 0.2$, $\theta_2 = 0.3$, $\varepsilon = 0.05$.

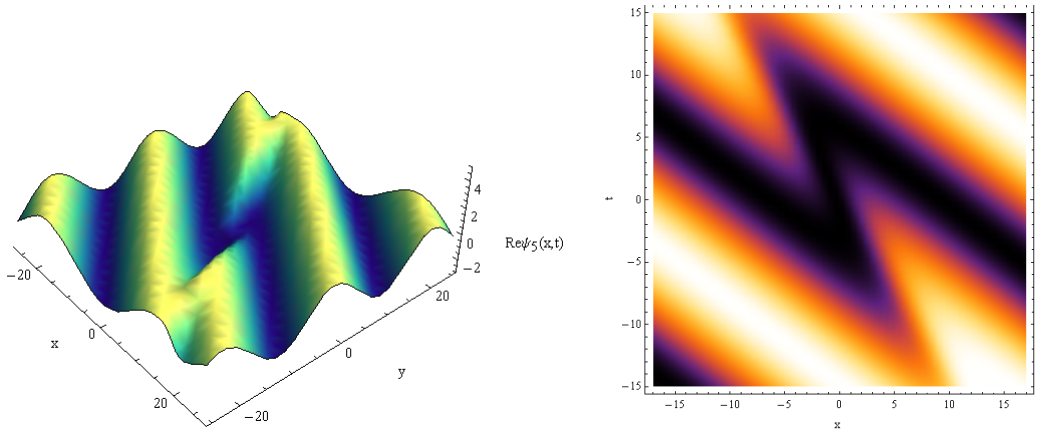

Figure 10. Real part of $\Psi_5(x,t)$ vs. x, y for $\alpha = 0.5$, $\rho_1 = 0.7$, $\rho_2 = 0.5$, $c_1 = 0.4$, $c_2 = 0.3$, $\theta_1 = 0.2$, $\theta_2 = 0.3$, $\varepsilon = 0.05$.

The effects of noise on the features of the solitary type solutions were investigated, which may be damped or grow with t. Equation (20) changes with t and the noise amplitude σ for a positive α value, as shown in Figure 11. It was shown that, by increasing σ, the dark envelope amplitudes decrease for the positive t axis and increase for the negative t axis, without changes of frequency, as seen in Figure 11.

For a negative α value, the same effect is produced with changes of the wave frequency, as in Figure 12. Moreover, solution (22) is plotted with time t and σ for a positive α value,

as shown in Figure 13. By increasing σ, the envelope solitary form was converted to a shock-forced oscillatory wave. For a negative α value, the amplitudes increased and the wave was converted to a huge bright periodic envelope wave, as in Figure 14.

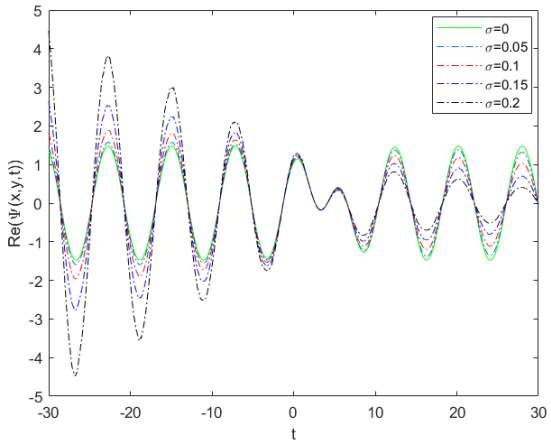

Figure 11. Real stochstic solution (20) vs. t, σ for $\alpha = 0.5$, $\rho_1 = 0.7$, $\rho_2 = 0.5$, $c_1 = 0.4$, $c_2 = 0.3$, $\theta_1 = 0.2, \theta_2 = 0.3, \varepsilon = 0.05$.

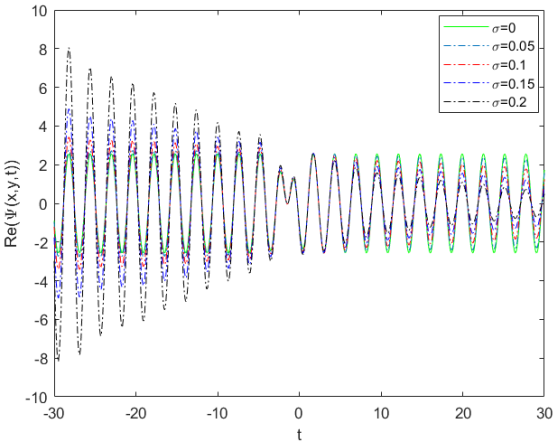

Figure 12. Real stochstic solution (20) vs. t, σ for $\alpha = -1.5$, $\rho_1 = 0.7$, $\rho_2 = 0.5$, $c_1 = 0.4$, $c_2 = 0.3$, $\theta_1 = 0.2, \theta_2 = 0.3, \varepsilon = 0.05$.

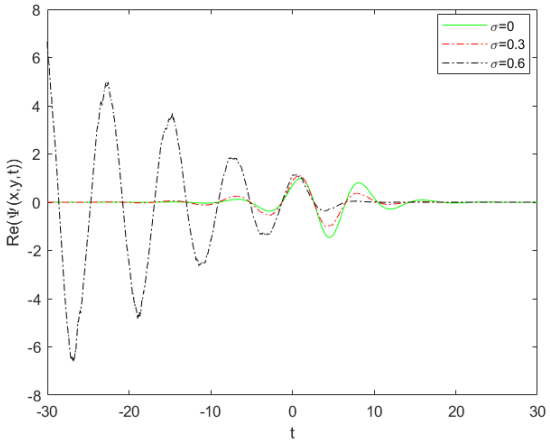

Figure 13. Real stochstic solution (22) vs. t, σ for $\alpha = 0.5$, $\rho_1 = 0.7$, $\rho_2 = 0.5$, $c_1 = 0.4$, $c_2 = 0.3$, $\theta_1 = 0.2, \theta_2 = 0.3, \varepsilon = 0.05$.

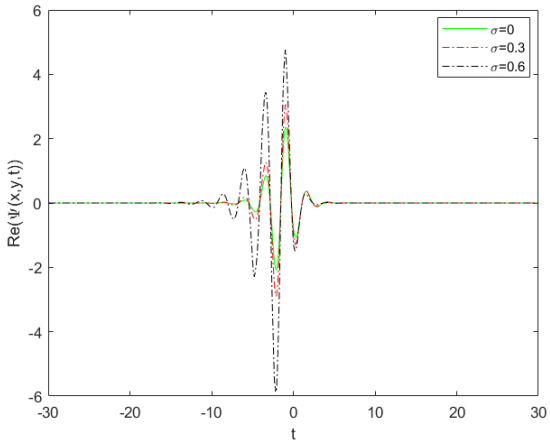

Figure 14. Real stochstic solution (22) vs. t, σ for $\alpha = -1.5$, $\rho_1 = 0.7$, $\rho_2 = 0.5$, $c_1 = 0.4$, $c_2 = 0.3$, $\theta_1 = 0.2$, $\theta_2 = 0.3, \varepsilon = 0.05$.

In view of the importance of the solutions found in this work, which give an accurate description of many types of solitary behavior, such as dark periodic envelopes, solitonic forms, bright solitons, and dissipative and dissipative–soliton-like waves, they demonstrate the accuracy of the solutions with a change of the values of the physical parameters of the studied system. This facilitates the process of comparison with previous studies. Our results are consistent with the dark and bright solutions in [18] in the case of an equation with constant coefficients, as well as the dark solutions and the dissipative solutions of [21]. In addition, our results are in agreement with [20], but the conception of the results in this work gives a distinctive description of the change of wave behaviors between the solitons, shocks, and the periodic forms for a change of system parameters, while neglecting noise strength. On the other hand, the noise strength produces shock-forced oscillatory behaviors and huge bright periodic envelope stochastic structures.

Remark 1.

1. *The solver proposed in this study can be applied to large classes of nonlinear stochastic partial differential equations (NSPDEs).*
2. *The suggested solver is simple to implement for solving stochastic fractional NPDEs.*

Remark 2. *Despite the fact that the suggested technique was implemented for all classes of NSPDEs that were transformed to Equation* (16)*, it failed to solve other classes of NSPDEs, which is regarded as a drawback of the proposed approach.*

5. Conclusions

A 2D stochastic CNLSE has been delivered using SGET. The CNLSE denoting the quantum fractional Hall effect edge states was solved utilizing SGET to describe solitary wave structures. New solutions for the absence of the noise term describe behaviors in the form of bright and dark periodic envelopes, and dissipative and dissipative–soliton-like waves, depending on the studied system's physical parameters. These solutions could be useful for quantum fractional Hall effect edge states. The effects of noise on the structural behavior of energy waves were investigated.The noise parameter σ modulated the wave attitude as amplitude variations, frequency fluctuations, and energy wave conversions. The present results may be important for Hall effect studies in quantum physics.

Author Contributions: H.G.A.: Conceptualization, Software, Formal analysis, Writing—original draft. A.F.A.: Conceptualization, Data curation, Writing—original draft. E.K.E.-S.: Conceptualization, Software, Formal analysis, Writing—review editing. M.A.E.A.: Conceptualization, Software, Formal analysis, Writing—review editing. All authors have read and agreed to the published version of the manuscript.

Funding: The authors extend their appreciation to the Deputyship for Research & Innovation, Ministry of Education in Saudi Arabia for funding this research work through project number (IF2/PSAU/2022/01/22803).

Data Availability Statement: Data sharing not applicable to this article, as no datasets were generated or analyzed during the current study.

Conflicts of Interest: The authors declare no conflict of interest.

References

1. Younis, M.; Ali, S.; Mahmood, S.A. Solitons for compound KdV Burgers equation with variable coefficients and power law nonlinearity. *Nonlinear Dyn.* **2015**, *81*, 1191–1196. [CrossRef]
2. Alharbi, A.; Almatrafi, M.B. Exact solitary wave and numerical solutions for geophysical KdV equation. *J. King Saud Univ.-Sci.* **2022**, *34*, 102087. [CrossRef]
3. Alharbi, A.R.; Abdelrahman, M.A.E.; Almatrafi, M.B. Analytical and numerical investigation for the DMBBM equation. *CMES-Comput. Model. Eng. Sci.* **2020**, *122*, 743–756. [CrossRef]
4. Abdelrahman, M.A.E.; Almatrafi, M.B.; Alharbi, A.R. Fundamental solutions for the coupled KdV system and its stability. *Symmetry* **2020**, *12*, 429. [CrossRef]
5. Abdelrahman, M.A.E.; Abdo, N.F. On the nonlinear new wave solutions in unstable dispersive environments. *Phys. Scr.* **2020**, *95*, 045220. [CrossRef]
6. Ullah, N.; Asjad, M.I.; Hussanan, A.; Akgül, A.; Alharbi, W.R.; Algarni, H.; Yahia, I.S. Novel waves structures for two nonlinear partial differential equations arising in the nonlinear optics via Sardar-subequation method. *Alex. Eng. J.* **2023**, *71*, 105–113. [CrossRef]
7. Biswas, A.; Konar, S. *Introduction to Non-Kerr Law Optical Solitons*; Chapman and Hall, CRC Press: Boca Raton, FL, USA, 2006.
8. Mirzazadeh, Q.Z.Q.M.; Ekici, M.; Sonmezoglu, A. Analytical study of solitons in non-Kerr nonlinear negative-index materials. *Nonlinear Dyn.* **2016**, *86*, 623–638.
9. Inc, M.; Aliyu, A.I.; Yusuf, A.; Bayram, M.; Baleanu, D. Optical solitons to the (n+1)-dimensional nonlinear Schrödinger's equation with Kerr law and power law nonlinearities using two integration schemes. *Mod. Lett. B* **2019**, *33*, 1950223. [CrossRef]
10. Kuo, C.K.; Ghanbari, B. Resonant multi-soliton solutions to new (3+1)-dimensional Jimbo-Miwa equations by applying the linear superposition principle. *Nonlinear Dyn.* **2019**, *96*, 459–464. [CrossRef]
11. Almatrafi, M.B.; Alharbi, A.; Tunç, C. Constructions of the soliton solutions to the good Boussinesq equation. *Adv. Differ. Equ.* **2020**, *2020*, 629. [CrossRef]
12. Shaikh, T.S.; Baber, M.Z.; Ahmed, N.; Shahid, N.; Akgül, A.; la Sen, M.D. On the soliton solutions for the stochastic Konno–Oono system in magnetic field with the presence of noise. *Mathematics* **2023**, *11*, 1472. [CrossRef]
13. Younis, M.; Rizvi, S.T.R. Dispersive dark optical soliton in (2+1)-dimensions by $(\frac{G'}{G})$-expansion with dual-power law nonlinearity. *Optik* **2015**, *126*, 5812–5814. [CrossRef]
14. Khodadad, F.S.; Nazari, F.; Eslami, M.; Rezazadeh, H. Soliton solutions of the conformable fractional Zakharov-Kuznetsov equation with dual-power law nonlinearity. *Opt. Quantum Electron.* **2017**, *49*, 384. [CrossRef]
15. Ashraf, R.; Ashraf, F.; Akgül, A.; Ashraf, S.; Alshahrani, B.; Mahmoud, M.; Weera, W. Some new soliton solutions to the (3+1)-dimensional generalized KdV-ZK equation via enhanced modified extended tanh-expansion approach. *Alex. Eng. J.* **2023**, *69*, 303–309. [CrossRef]
16. Li, B.Q. Phase transitions of breather of a nonlinear Schrödinger equation in inhomogeneous optical fiber system. *Optik* **2020**, *217*, 164670. [CrossRef]
17. Li, B.Q.; Ma, Y.L. Extended generalized Darboux transformation to hybrid rogue wave and breather solutions for a nonlinear Schrödinger equation. *Appl. Math. Comput.* **2020**, *386*, 125469. [CrossRef]
18. Biswas, A. chiral solitons in 1+2 dimensions. *Int. J. Theor. Phys* **2009**, *48*, 3403–3409. [CrossRef]
19. Alharbi, Y.F.; El-Shewy, E.K.; Abdelrahman, M.A.E. Effects of Brownian noise strength on new chiral solitary structures. *J. Low Freq. Noise Vib. Act. Control.* **2022**, *42*. [CrossRef]
20. Javid, A.; Raza, N. Chiral solitons of the (1 + 2)-dimensional nonlinear Schrödinger's equation. *Mod. Phys. Lett. B* **2019**, *33*, 1950401. [CrossRef]
21. Eslami, M. Trial solution technique to chiral nonlinear Schrödinger's equation in(1+2)-dimensions. *Nonlinear Dyn.* **2016**, *85*, 813–816. [CrossRef]
22. Alomair, R.A.; Hassan, S.Z.; Abdelrahman, M.A.E. A new structure of solutions to the coupled nonlinear Maccari's systems in plasma physics. *AIMS Math.* **2022**, *7*, 8588–8606. [CrossRef]
23. Samadyar, N.; Ordokhani, Y.; Mirzaee, F. The couple of Hermite-based approach and Crank-Nicolson scheme to approximate the solution of two dimensional stochastic diffusion-wave equation of fractional order. *Eng. Anal. Bound. Elem.* **2020**, *118*, 285–294. [CrossRef]
24. Almatrafi, M.B. Solitary wave solutions to a fractional model using the improved modified extended tanh-function method. *Fractal Fract.* **2023**, *7*, 252. [CrossRef]

25. Mirzaee, F.; Samadyar, N. Numerical solution of time fractional stochastic Korteweg-de Vries equation via implicit meshless approach. *Iran. J. Sci. Technol. Trans. A Sci.* **2019**, *43*, 2905–2912. [CrossRef]
26. Mirzaee, F.; Rezaei, S.; Samadyar, N. Numerical solution of two-dimensional stochastic time-fractional sine-Gordon equation on non-rectangular domains using finite difference and meshfree methods. *Eng. Anal. Bound. Elem.* **2021**, *127*, 53–63. [CrossRef]
27. Almatrafi, M.B.; Alharbi, A. New soliton wave solutions to a nonlinear equation arising in plasma physics. *Comput. Model. Eng. Sci.* **2023**, *137*, 827–841. [CrossRef]
28. Samadyar, N.; Ordokhani, Y.; Mirzaee, F. Hybrid Taylor and block-pulse functions operational matrix algorithm and its application to obtain the approximate solution of stochastic evolution equation driven by fractional Brownian motion. *Commun. Nonlinear Sci. Numer. Simul.* **2020**, *90*, 105346. [CrossRef]
29. Dalfovo, F.; Giorgini, S.; Pitaevskii, L.P.; Stringari, S. Theory of Bose-Einstein condensation in trapped gases. *Rev. Mod. Phys.* **1999**, *71*, 463. [CrossRef]
30. Nakkeeran, K. Bright and dark optical solitons in fiber media with higher-order effects. *Chaos Solitons Fractals* **2002**, *13*, 673–679. [CrossRef]
31. Abdelrahman, M.A.E.; Sohaly, M.A.; Alharbi, Y.F. Fundamental stochastic solutions for the conformable fractional NLSE with spatiotemporal dispersion via exponential distribution. *Phys. Scr.* **2021**, *96*, 125223. [CrossRef]
32. Mirzaee, F.; Sayevand, K.; Rezaei, S.; Samadyar, N. Finite difference and spline approximation for solving fractional stochastic advection-diffusion equation. *Iran. J. Sci. Technol. A Sci.* **2021**, *45*, 607–617. [CrossRef]
33. Nishino, A.; Umeno, Y.; Wadati, M. Chiral nonlinear Schrödinger equation. *Chaos Solitons Fractals* **1998**, *9*, 1063–1069. [CrossRef]
34. Tsitsas, N.L.; Lakhtakia, A.; Frantzeskakis, D.J. Vector solitons in nonlinear isotropic chiral metamaterials. *J. Phys. A Math. Theor.* **2011**, *44*, 435203. [CrossRef]
35. Ismail, M.S.; Al-Basyouni, K.S.; Aydin, A. Conservative finite difference schemes for the chiral nonlinear Schrödinger equation. *Bound. Value Probl.* **2015**, *89*, 2015. [CrossRef]
36. Younis, M.; Cheemaa, N.; Mahmood, S.A.; Rizvi, S.T.R. On optical solitons: The chiral nonlinear Schrödinger equation with perturbation and Bohm potential. *Opt. Quant. Electron.* **2016**, *48*, 542. [CrossRef]
37. Yan, C. A simple transformation for nonlinear waves. *Phys. Lett. A* **1996**, *224*, 77–84. [CrossRef]
38. Karatzas, I.; Shreve, S.E. *Brownian Motion and Stochastic Calculus*, 2nd ed.; Springer: Berlin/Heidelberg, Germany, 1991.
39. ∅ksendal, B. *Stochastic Differential Equations: An Introduction with Applications*, 6th ed.; Springer: Berlin/Heidelberg, Germany, 2003.
40. Griguolo, L.; Seminara, D. Chiral solitons from dimensional reduction of Chern-Simons gauged nonlinear Schrödinger equation: Classical and quantum aspects. *Nucl. Phys. B* **1998**, *516*, 467–498. [CrossRef]
41. Lee, J.H.; Lin, C.K.; Pashev, O.K. Shock waves, chiral solitons and semi-classical limit of one-dimensional anyons. *Chaos Solitons Fractals* **2004**, *19*, 109–128. [CrossRef]
42. Aglietti, U.; Griguolo, L.; Jackiw, R.; Pi, S.Y.; Semirara, D. Anyons and Chiral Solitons on a Line. *Phys. Rev. Lett.* **1996**, *77*, 44064409. [CrossRef]